Sharifzadeh M, (2013). Implementation of an inversely controlled process model for integrated design and control of an ETBE reactive distillation, Chemical Engineering Science. 92, 21–39.

Implementation of a steady-state inversely controlled process model for integrated design and control of an ETBE reactive distillation

Mahdi Sharifzadeh[a,*]

[a] Centre for Process System Engineering (CPSE), Department of Chemical Engineering, Imperial College London,

Abstract

Recently, Sharifzadeh and Thornhill (2012) proposed a modeling approach for control structure selection using an inversely controlled process model, which benefits from significant complexity reductions. The treatment was based on the property that the inverse solution of a process model determines the best achievable control performance. The present article applies that methodology for integrated design and control of an ethyl tert-butyl ether (ETBE) reactive distillation column. In addition, the simulation-optimization program is reformulated using a penalty function, resulting in less optimization variables and better convergence of the simulation program. While the required computational efforts remain almost at the same level of steady-state process optimization, the process and its control structure are optimized simultaneously and regulatory steady-state operability of the solution is ensured. Finally, dynamic simulation is applied for detailed design of PI control loops.

Keywords:

Systems engineering, Process control, Optimization, Simulation, Integrated design and control, Perfect control

[*] Correspondence concerning this article should be addressed to Mahdi Sharifzadeh; email:mahdi@imperial.ac.uk; address: Department of Chemical Engineering, Imperial College London, South Kensington Campus, London, UK, SW7 2AZ.

1. Introduction

The conventional approach to integrated design and control is to optimize the process and its controllers simultaneously. However, there are several numerical as well as conceptual complexities associated with optimization of controllers. Firstly, including controllers in the integrated design and control framework requires decision-making regarding the degree of centralization (and in the case of decentralized control structures, pairing/partitioning between manipulated and controlled variables), the type of controllers (e.g., feedback, feed forward, model based), and the controller parameters, which increases the size of the problem several orders of magnitude. Secondly, controllability and operability are the inherent properties of the process and its control structure and do not depend on controller design. For example, it is not possible to resolve the inoperability issue of a process by changing the design of its controllers. Finally, optimizing the controllers is of limited practicality, because the modern control systems are often designed during commissioning stages and using commercial packages which may not be available at process design stages.

The desire for a controller-independent method, which only needs steady-state information, is also emphasized by other researchers. For example, the following excerpt from Bogle, et al, (2004) explains the motivations for steady-state multiplicity analysis:

"… it is desirable that a method should be one that only uses open loop steady state data while considering dynamic characteristics of a process design, i.e. information that is independent of a detailed controller design, and could eliminate the design candidates for which a controller that achieves the control objectives in the face of disturbances does not exist, whatever controller design method is used"

Other examples of the steady-state methods include self-optimizing control strategy (Skogestad, 2000), steady-state operability analysis (Georgakis, et al. 2003) and static relative gain array (sRGA) and its variants (e.g., Moaveni and Khaki-Sedigh, 2009).

Motivated by the complexity reduction incentives, Sharifzadeh and Thornhill (2012; 2013) proposed a new modeling approach using the so-called *inversely controlled process model*. The new development is based on the property that inverse solution of the process model can be employed for evaluating the

best achievable control performance and hence implies perfect control. The advantage of applying an inversely controlled process model is that all the aforementioned numerical and conceptual complexities associated with detailed design of controllers are disentangled from the problem formulation. However, the process and its control structure are still optimized simultaneously. Then, detailed controller design will be performed for the optimized process and control structure.

Sharifzadeh and Thornhill (2012) proposed a steady-state inversely controlled process model for selecting the control structure of an industrial distillation train. The inversion of the process model was made by selecting the specifications (degrees of freedom) of the process simulation according to the candidate controlled and manipulated variables. In this article, similar methodology is implemented for integrated design and control of an ethyl tert-butyl ether (ETBE) reactive distillation column. However, the simulation-optimization program is modified by including a penalty function and unlike the formulation of Sharifzadeh and Thornhill (2012), it is not necessary to strictly satisfy the perfect control constraints at each optimization iteration. Therefore, in the new formulation, the choices of the simulation specifications are no longer restricted to the candidate controlled and manipulated variables, resulting in better convergence of the simulation program and significantly less binary optimization variables. Finally, it will be shown that the applied method ensures the regulatory steady-state operability of the designed process and control structure.

The paper is organized in three parts. In the first part, the theory of research is presented. The mathematical formulation of the applied integrated design and control framework is developed by modifying the previous mathematical formulation presented by Sharifzadeh and Thornhill (2012). It is also shown that the applied method ensures regularity steady-state operability. In addition, it is explained that since dynamic degrees of freedom (representing material inventories) do not appear in a steady-state model, their implications should be considered before optimization in order to ensure that the results are consistent with the requirements of the inventory control systems. The second part of this paper applies the optimization framework for integrated design and control of an ethyl tert-butyl ether (ETBE) reactive distillation column. The process description is presented. Then, the discussions go on with explaining the instances of the goal-driven multi-objective function for the

case study and justification of its target values. In addition, the optimization variables and constraints are formulated and discussed and the applied optimization and modeling tools are reported and explained. Finally, the third part of the paper presents and discusses the results. These include a comparison between the modeling approaches based on kinetic correlations and equilibrium assumptions, the results of integrated design and control based on perfect control and detailed design of controllers using dynamic simulation.

2. Theory

This part of the paper presents the theory of the research. The features of interest are modification of the mathematical formulation of the method using a penalty function and a discussion regarding the steady-state operability of the solution. In addition, the goal programming multi-objective function and implications of the inventory control systems are discussed briefly.

2.1. Mathematical formulation

Sharifzadeh and Thornhill (2012) presented the mathematical formulation of optimal control structure selection using a steady-state inversely controlled process model (Problem II of that publication). The equivalent mathematical formulation for integrated design and control can be constructed by including the process structural and parametric decisions, as well as the setpoints of the candidate controlled variables and the nominal values of the candidate manipulated variables, as follows:

$$\min E\{J_s[\boldsymbol{Y_p}, \boldsymbol{Y_{CV}}, \boldsymbol{Y_{MV}}, \boldsymbol{p}, \boldsymbol{y_{setpoint}}, \boldsymbol{u_{nominal}}]\} \qquad \text{Problem 1}$$

subject to:

$$\boldsymbol{h}[\boldsymbol{x}, \boldsymbol{u}, \boldsymbol{y}, \boldsymbol{Y_p}, \boldsymbol{p}, \boldsymbol{\mu}] = 0$$

$$\boldsymbol{g}[\boldsymbol{x}, \boldsymbol{u}, \boldsymbol{y}, \boldsymbol{Y_p}, \boldsymbol{p}, \boldsymbol{\mu}] \leq 0$$

$$\Omega_s[\boldsymbol{\mu}] = 0$$

$$Y_{CV,i} \times (y_i - y_{i,setpoint}) = 0 \qquad i \in I_{CV}$$

$$(1 - Y_{MV,j}) \times (u_j - u_{j,nominal}) = 0 \qquad j \in I_{MV}$$

$$\boldsymbol{\psi}(Y_{CV,i}, Y_{MV,j}) \geq 0$$

In above, $\boldsymbol{x}$ is the vector of process variables, $\boldsymbol{u}$ is the vector of candidate manipulated variables, $\boldsymbol{y}$ is

97 the vector of candidate controlled variables, $\boldsymbol{p}$ is the vector of process parameters, $\boldsymbol{\mu}$ is the vector of
98 disturbance parameters. s is the index of disturbance scenarios. $\boldsymbol{Y_p}$ is the vector of structural process
99 variables. $\boldsymbol{Y_{CV}}$ and $\boldsymbol{Y_{MV}}$ are the vectors of structural variables for selection of controlled and
100 manipulated variables respectively. While $\boldsymbol{Y_p}$, $\boldsymbol{Y_{CV}}$ and $\boldsymbol{Y_{MV}}$ are the vectors of integer variables, the
101 rest of the variables are continuous. In addition, $\boldsymbol{h}[\,] = 0$ is the vector of equality constraints, $\boldsymbol{g}[\,] \leq 0$
102 is the vector of inequality constraints, $\boldsymbol{\Omega}[\,] = 0$ is the vector of the equations for disturbances. The
103 expected value $E\{\,\}$ of the objective function $J_s[\,]$ should be minimized.
104 In this research, it is assumed that the critical disturbance scenarios are known in advance. However,
105 if it is not the case or the process is prone to other uncertainties such as the uncertainties in the model
106 parameters, the method of steady-state flexibility optimization can be combined with the present
107 formulation, (Grossmann and Floudas 1987). This method adds an external optimization loop to the
108 problem in which the violations of constraints are maximized with respect to the uncertain parameters.
109 Then in each iteration of the optimization procedure, the current worst scenario is identified and
110 added to the set of the critical uncertain scenarios. The iterations of the two optimization loops
111 continue until there is no value of the uncertain parameters for which the constraints are violated.
112 In Problem 1, the following perfect control constraints replaced the controller model:

$$Y_{CV,i} \times \left(y_i - y_{i,setpoint}\right) = 0 \qquad i \in I_{CV} \qquad (1a)$$

$$(1 - Y_{MV,j}) \times \left(u_j - u_{j,nominal}\right) = 0 \qquad j \in I_{MV} \qquad (1b)$$

113 where y_i represents a candidate controlled variable and $y_{i,setpoint}$ is the corresponding setpoint. In
114 addition, u_j represents a candidate manipulated variable and $u_{j\prime,nominal}$ is the corresponding nominal
115 value. The implication of equation $(1b)$ is that if a manipulated variable is not selected, it will be left
116 unadjusted at its nominal value. The constraints $\boldsymbol{\psi}() \geq 0$ ensure that the selected controlled and
117 manipulated variables are consistent with the available degrees of freedom and the requirements of
118 inventory control. I_{CV} and I_{MV} are the index sets of the candidate controlled and manipulated variables
119 respectively.
120 In Introduction Section, the conceptual and numerical complexities associated with including
121 controllers in the problem formulation were discussed. Generally, constructing a mathematical

superstructure that includes all the alternative control loops between the candidate controlled and manipulated variables and provides the decision-making opportunity for pairing/partitioning of these variables, increases the size of the problem by several orders of magnitude. Investigating the formulation of Problem 1 suggests that the controller superstructure is replaced by perfect control equations. As a result, the size of Problem 1 is significantly smaller than the conventional formulation including a controller superstructure. Furthermore, while including controllers requires dynamic optimization, Problem 1 is significantly less computational intensive due to its steady-state formulation. Finally, it is not necessary anymore to select the type of the controllers in advance.

However, the formulation of Problem 1 still suffers from combinatorial complexities, because for each candidate controlled and manipulated variable, a binary optimization variable is needed (i.e., $Y_{CV,i}$ and $Y_{MV,j}$). Furthermore, for each combination of the candidate controlled and manipulated variables, an inversely controlled process model needs to be constructed (e.g., see Section 3.3.3 and Figure 4 of (Sharifzadeh and Thornhill 2012)). In this paper, in order to overcome these difficulties, the following penalty function is introduced, which replaces the perfect control constraints (1a, b) in Problem 1:

$$\text{Penalty} = \sum_{d=1}^{\text{DOF}} w'_c \times \text{sort}_d \{\text{Dev}_c\} \qquad c \in I_{CV} \cup I_{MV} \qquad (2a)$$

$$\text{Dev}_i = \sum_{s=1}^{Ns} \left| \frac{y_{i,s} - y_{i,desired}}{y_{i,desired}} \right| \qquad i \in I_{CV} \qquad (2b)$$

$$\text{Dev}_j = \sum_{s=1}^{Ns} \left| \frac{u_{j,s} - u_{nominal}}{u_{nominal}} \right| \qquad j \in I_{MV} \qquad (2c)$$

In above, DOF is the number of available degrees of freedom and N_s is the number of disturbance scenarios. Dev_i is the deviation of candidate controlled variable i from its desired setpoint for all disturbance scenarios. Dev_j is the deviation of candidate manipulated variable j from its nominal value for all disturbance scenarios. In addition, w'_c is the weighting factor of the deviation variables in the penalty function. In analogy to equation (1b), the manipulated variable that its deviation variable is ranked by the $sort$ operator is not selected. The total number of the selected controlled

variables and the unselected manipulated variables is equal to the total number of the available degrees of freedom (i.e., DOF). In addition, the deviation variables in equations (2b) and (2c) are scaled and they have different weighting factors in equation (2a). The reason is that different controlled and manipulated variables have different dimensions. Therefore, the corresponding weighting factors, w'_c should be strong enough, so by convergence of the optimization procedure, the final values of the deviation variables corresponding to the selected controlled variables and the unselected manipulated variables will be negligible. For example, for a temperature controlled variable, a deviation value less than 10^{-3} K ensures that this variable is almost perfectly controlled.

In each iteration of the optimization procedure, the deviation variables Dev_i and Dev_j are calculated for all disturbance scenarios. Then, the manipulated and controlled variables corresponding to the least deviations are selected and their deviations are penalized. In other words, by minimizing the penalty function, the optimization procedure tries to choose the controlled and manipulated variables. Furthermore, since the penalty function and the main objective function (to be discussed in Section 2.3) are minimized simultaneously, these choices of controlled and manipulated variables are also optimal with respect to the main objective function. In conclusion, the new formulation is as follows:

$$\min E\{J_s[\boldsymbol{Y_p}, \boldsymbol{p}, \boldsymbol{y_{setpoint}}, \boldsymbol{u_{nominal}}]\} + \text{Penalty} \qquad \text{Problem 2}$$

subject to:

$$\boldsymbol{h}[\boldsymbol{x}, \boldsymbol{u}, \boldsymbol{y}, \boldsymbol{Y_p}, \boldsymbol{p}, \boldsymbol{\mu}] = 0$$

$$\boldsymbol{g}[\boldsymbol{x}, \boldsymbol{u}, \boldsymbol{y}, \boldsymbol{Y_p}, \boldsymbol{p}, \boldsymbol{\mu}] \leq 0$$

$$\Omega_s[\boldsymbol{\mu}] = 0$$

$$\boldsymbol{\psi}(Y_{CV,i}, Y_{MV,j}) \geq 0$$

The formulation of Problem 2 has several advantages over the formulation of Problem 1:

- Firstly, in the new formulation, there is no need to optimize the binary variables of the candidate controlled and manipulated variables (i.e., $Y_{cv,i}$, $Y_{mv,j}$ in Problem 1). The values of these binary variables are deduced from the ranking of the deviation variables, as explained earlier. This strategy significantly reduces the number of the optimization variables, because the number of the candidate manipulated and controlled variables potentially can be very

large. By comparison, only a few of them will eventually be selected as controlled and manipulated variables.

- Secondly, unlike the first formulation, it is not needed to construct an inversely controlled process model in each optimization iteration and the process model inversion will be ensured by convergence of the optimization algorithm due to minimization of the penalty function. As a result, the choices of the simulation specifications are not restricted to the selected controlled and manipulated variables. This is an important advantage because convergence of the simulation program for some inverse models can be poor.
- Thirdly, it is well known that the main barrier for integrated design and control is the formidable computational costs and the high level of the required expertise in dynamic mathematical modeling and optimization. Therefore, the current industrial practice has a sequential approach in which firstly, the process is optimized with respect to a steady-state economic objective function and then the process design specifications are used for control design. Such an approach is unfortunate because when the process design is fixed, there is little room left for improving the control performance. Nevertheless, investigating Problem 2 suggests that while the required computational and modeling efforts remain similar to steady-state process optimization, the process and its control structure are optimized simultaneously. In addition, as will be discussed in the next section, the applied method ensures regulatory steady-state operability of the solution.

2.2. Regulatory steady-state operability

Sharifzadeh and Thornhill (2012) suggested that the application of a steady-state inversely controlled process model ensures state controllability. Unfortunately, that claim does not always hold. The reason is that not all the states (e.g., liquid hold-up) appear in a steady-state formulation. A more rigorous evaluation can be based on regulatory steady-state operability, as discussed in the following. Georgakis, et al. (2003) introduced regulatory steady-state operability index as the fraction of the desired input set which is available:

$$\mathrm{r-OI} = \frac{\sigma\left(\mathrm{AIS} \cap \mathrm{DIS}_{\mu}\left(\boldsymbol{y}_{setpoint}\right)\right)}{\sigma\left(\mathrm{DIS}_{\mu}\left(\boldsymbol{y}_{setpoint}\right)\right)} \qquad (3a)$$

where the desired input set, $\mathrm{DIS}_{\mu}\left(\boldsymbol{y}_{setpoint}\right)$, is defined as:

$$\mathrm{DIS}_{\mu}\left(\boldsymbol{y}_{setpoint}\right) = \{u |\, d\boldsymbol{x}/dt = 0, d\boldsymbol{u}/dt = 0, \boldsymbol{y} = \boldsymbol{y}_{setpoint}; \forall \mu \in \mathrm{EDS}\} \qquad (3b)$$

In above, AIS represents the available input set which are the values that the input (manipulated) variables are able to take and EDS represents the expected disturbance space. σ is a measure of the size of each set, e.g., in a two-dimensional space, it represents the area and in a three-dimensional space, it represents the volume, and so on. Notice that the desired input set $\mathrm{DIS}_{\mu}\left(\boldsymbol{y}_{setpoint}\right)$, is the function of both expected disturbances, μ , and desired setpoints, $\boldsymbol{y}_{setpoint}$.

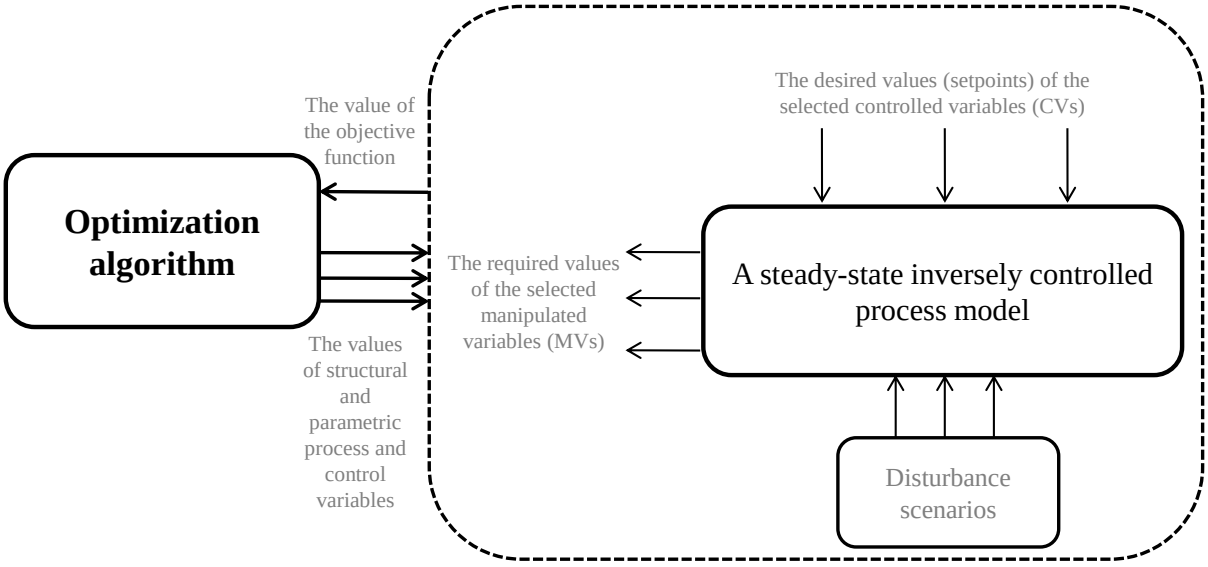

Fig. 1. Integrated design and control using a steady-state inversely controlled process model (adapted from Sharifzadeh and Thornhill 2012 with permission).

A comparison between the information flow in the-applied steady-state framework and the definition of regulatory steady-state operability is illustrative. Fig. 1, adapted from Sharifzadeh and Thornhill (2012), shows that in each iteration of the optimization framework, for each disturbance, $\forall \mu \in$ EDS, the desired input set $\mathrm{DIS}_{\mu}\left(\boldsymbol{y}_{setpoint}\right)$ is calculated in order to maintain the controlled variables at their setpoints, $\boldsymbol{y}_{setpoint}$,. If no constraint on the input (manipulated) variables is violated, the whole set of

207 $\mathrm{DIS}_{\mu}(\boldsymbol{y}_{setpoint})$ will be achievable and this set is identical with AIS. Therefore, the regulatory steady-
208 state operability index will be equal to one. Otherwise, if any constraint on input variables is violated,
209 the optimization framework has encountered an infeasible solution and will be redirected to the
210 feasible solutions for which the regulatory steady-state operability is equal to one.

211 *2.3. Multi-objective function and goal programming*

212 The applied objective functions in this research were presented and justified by Sharifzadeh and
213 Thornhill (2012) and are listed in Table 1 adapted from that publication. Similar to the previous
214 research, this paper also applies goal programming. In goal programming, each objective function is
215 given a goal or target value. The deviations from these target values are used to construct an
216 aggregated objective value as follows:

$$J_s = \left(\frac{1}{4} \times \sum_{k=1}^{4} w_k \times \left|\frac{Obj_{k,s} - {Obj_k}^{target}}{{Obj_k}^{target}}\right| + Maximum\left\{w_k \times \left|\frac{Obj_{k,s} - {Obj_k}^{target}}{{Obj_k}^{target}}\right|\right\}\right), \quad k = 1 \ldots 4 \tag{4}$$

217 where s is the index of disturbances. The objective function (4) applies the efficiency-equity trade-off
218 method in which both the average of the deviational variables and their maximum are considered
219 simultaneously, (Jones and Tamiz 2010). w_k are the weighting factors of different objectives.
220 It is notable that in general, the solution of a multi-objective optimization is a set of Pareto-efficient
221 solutions. One way of constructing this set is to vary the weighting factors and solving the
222 optimization problem for each combination of them. However, constructing such a 4-D Pareto front
223 can be infeasible for many practical problems. Therefore, in this research the values of the weighting
224 factors, w_k , are chosen in such a way that the terms in equation (4) have the same orders of
225 magnitude. This is because, as Jones and Tamiz (2010) argued, the underlying philosophy of goal
226 programming is "*satisfying*" and "*sufficiency*" of the achieved level of the targets. Otherwise, a
227 solution for which all the targets are met is often infeasible.
228

Table 1

Objective functions for steady-state integrated design and control adapted from (Sharifzadeh and Thornhill 2012) with permission.

Obj_1 = the deviations in the quality and quantity of products (inferential controlled variables)
Obj_2 = the deviations in the manipulated variables
Obj_3 = the deviations in the state variables
Obj_4 = the economic losses due to disturbances

Goal programming of the first three objectives in Table 1 poses no difficulty because ideally the deviations in the inferential controlled variables, the changes in the manipulated variables and the deviations in the state variables must be minimized toward zero. These objectives will ensure tight control of the process. However, for the fourth objective in Table 1, a target is needed to ensure optimal profitability. This target can be determined by maximizing Total Annual Profit, as will be explained later in Case Study Section. The deviations of all the objective functions from their target values are minimized toward zero:

$$Obj_{k,s} - Obj_k^{\,target} \rightarrow 0 \qquad k = 1 \dots 4 \tag{5}$$

Then, the expected value of the aggregated objective function for different disturbance scenarios must be minimized. The expected value can be constructed by summing up the objective values weighted by the likelihood of each disturbance scenario, L_s (Sahinidis 2004):

$$min \sum_{s=1}^{n_s} L_s \times J_s\left[\boldsymbol{Y_p}, \boldsymbol{p}, \boldsymbol{y_{setpoint}}, \boldsymbol{u_{nominal}}\right] + \text{Penalty} \qquad \text{Problem 2. gp}$$

subject to:

$$\boldsymbol{h}[\boldsymbol{x}, \boldsymbol{u}, \boldsymbol{y}, \boldsymbol{Y_p}, \boldsymbol{p}, \boldsymbol{\mu}] = 0$$

$$\boldsymbol{g}[\boldsymbol{x}, \boldsymbol{u}, \boldsymbol{y}, \boldsymbol{Y_p}, \boldsymbol{p}, \boldsymbol{\mu}] \leq 0$$

$$\Omega_s[\boldsymbol{\mu}] = 0$$

$$\boldsymbol{\psi}(Y_{CV,i}, Y_{MV,j}) \geq 0$$

Addressing Problem 2.gp, using simulation-optimization programming will be demonstrated for a reactive distillation column in the second part of this paper.

2.4. *Inventory control systems*

The controlled variables concerning material inventories (e.g., the levels of liquid inventories or the pressures representing gaseous inventories) do not appear in a steady-state model. However, as emphasized by other researchers (e.g., Huang, et al. 2012) too, the available manipulated variables are shared between inventory controlled variables and steady-state controlled variables. Therefore, a pre-optimization analysis is needed, as discussed by Sharifzadeh and Thornhill (2012). The aim of this analysis is to ensure that after optimization, all the required manipulated variables are available and no inventory controlled variable is left uncontrolled. The instance of this analysis will be presented later for a reactive distillation column.

2.5. *The limitations of a steady-state inversely controlled process model*

The applied method using a steady-state inversely controlled process model is limited to continuous processes, and is not applicable to processes with dynamic natures such as batch or semi-continuous processes. In addition, the integrating variables, (e.g. liquid hold-up) do not appear in a steady-state model. The steady-state inversely controlled process model considers only the initial and final states of the process and it has no implication for the transient states between the initial and final states. These observations suggest that a more thorough analysis requires constructing a dynamic inversely controlled process model, which is studied elsewhere (Sharifzadeh and Thornhill 2013). However, as recognized by other researchers (e.g., Malcolm, et al., 2007), dynamic integrated design and control is a tough challenge for current optimization technologies and the problems that can be solved rigorously using dynamic optimization are smaller. Therefore, a method that can at least screen the promising solutions for further dynamic analysis is highly desirable.

In addition, Sharifzadeh and Thornhill (2013) argued that since dynamic inversion has a direct relationship with functional controllability, their proposed method captures and avoids the adverse effects of control imperfections. The causes of control imperfection are the constraints on manipulated variables, model uncertainties, time delays, and non-minimum phase behavior. Since the applied steady-state method only considers initial and final states, for highly nonlinear processes with the risk of violating the manipulated variable constraints during the transient states, (i.e., path constraints), the

steady-state analysis will be insufficient. In addition, it was explained earlier (Section 2.1) that the worst scenarios for steady-state uncertainties can be identified using steady-state flexibility optimization. However, dynamic uncertainties such as time-varying disturbances (see Dimitriadis and Pistikopoulos 1995) cannot be captured by a steady-state model. Moreover, time delays do not appear in a steady-state model. Finally, unstable zero dynamics are nonlinear analogues of right-half-plane zeros and imply instability of the process inversion, called non-minimum phase behavior (Slotine & Li, 1991). For example, input-multiplicity, a scenario in which several inputs produce the same output, causes non-minimum phase behavior, (Bogle, et al. 2004). Although steady-state methods are developed for multiplicity analysis, studying the other causes of control imperfection requires dynamic modeling. Therefore, in this research, the results of the applied method using a steady-state inversely controlled process model are evaluated in a post-optimization analysis using dynamic simulation.

3. Case study

In this part of the paper, the reformulated optimization framework for integrated design and control is applied to an ETBE reactive distillation column. Reactive distillations are the leading technologies for process intensification. The application of these processes is motivated by significant reductions in the required investment capital and operating costs compared to the equivalent conventional reaction-separation processes. Furthermore, reactive distillations have significant advantages when conversion is thermodynamically limited by chemical equilibrium. The reason is that continuous removal of the products drives the overall conversion to completion. Other benefits include reduced downstream processing and higher energy efficiency due to utilization of the reaction heat for evaporation of the liquid phase (Sharma and Singh 2010). A comprehensive review of the industrial applications of reactive distillations is provided by Sundmacher and Kienle (2003).

Table 2 lists some representative studies in the field. As shown in this table, a wide spectrum of methods is proposed by researchers, which includes shortcut and graphical methods, multiplicity analysis, control structure selection, detailed design of controllers, and simultaneous optimization of process design and control. In the subsequent sections, the reformulated optimization framework for

integrated design and control using a steady-state inversely controlled process model is applied to the case of an ETBE reactive distillation column.

Table 2

A representative list of research in the field of reactive distillation design and control

Study	Focus	Method
Avami, et al. (2012); Barbosa and Doherty (1988); Carrera-Rodríguez, et al. (2011); Dragomir and Jobson (2005)	Process design	Graphical tools and short-cut methods
Cardoso, et al. (2000); Jackson and Grossmann (2001)	Process design	Optimization
Lee, et al. (2010); Zhu, et al. (2009).	Heat integration	Simulation
Bisowarno, et al. (2003); Khaledi and Young (2005); Sneesby, et al. (2004);	Controller design	Simulation
Al-Arfaj and Luyben, (2002); Al-Arfaj and Luyben (2004); Huang, et al. (2012); Luyben (2005)	Control structure selection	Simulation
Ramzan, et al. (2010); Guttinger and Morari (1999a, b).	Steady-state multiplicity analysis	Simulation
Babu, et al. (2009); Georgiadis, et al. (2002); Miranda, et al. (2008); Panjwani, et al. (2005)	Integrated design and control	Optimization

3.1. Process description

There is an increasing demand for ethyl tert-butyl ether (ETBE), as a gasoline oxygenate and octane enhancer, and it is replacing methyl tert-butyl ether (MTBE) due to environmental concerns of the latter. In addition, ETBE is produced from reaction of isobutene and ethanol, and hence is semi-renewable (Al-Arfaj and Luyben 2002):

$$C_4H_8\,(isobutene) + C_2H_6O\,(ethanol) \leftrightarrow C_6H_{14}O\,(ETBE) \quad (6)$$

This reaction is equilibrium limited (only 84.7% at 70 ^{o}C). The process flow diagram of an ETBE reactive distillation column is shown in Fig. 2. The C4s feed stream is a mixture of isobutene and n-butene. N-butene is an inert and does not participate in the reaction. The distillate is mainly n-butene and the bottom stream is mainly ETBE. If the reactants are not fed according to the stoichiometry of the reaction, the excess ethanol leaves the column in the bottom stream.

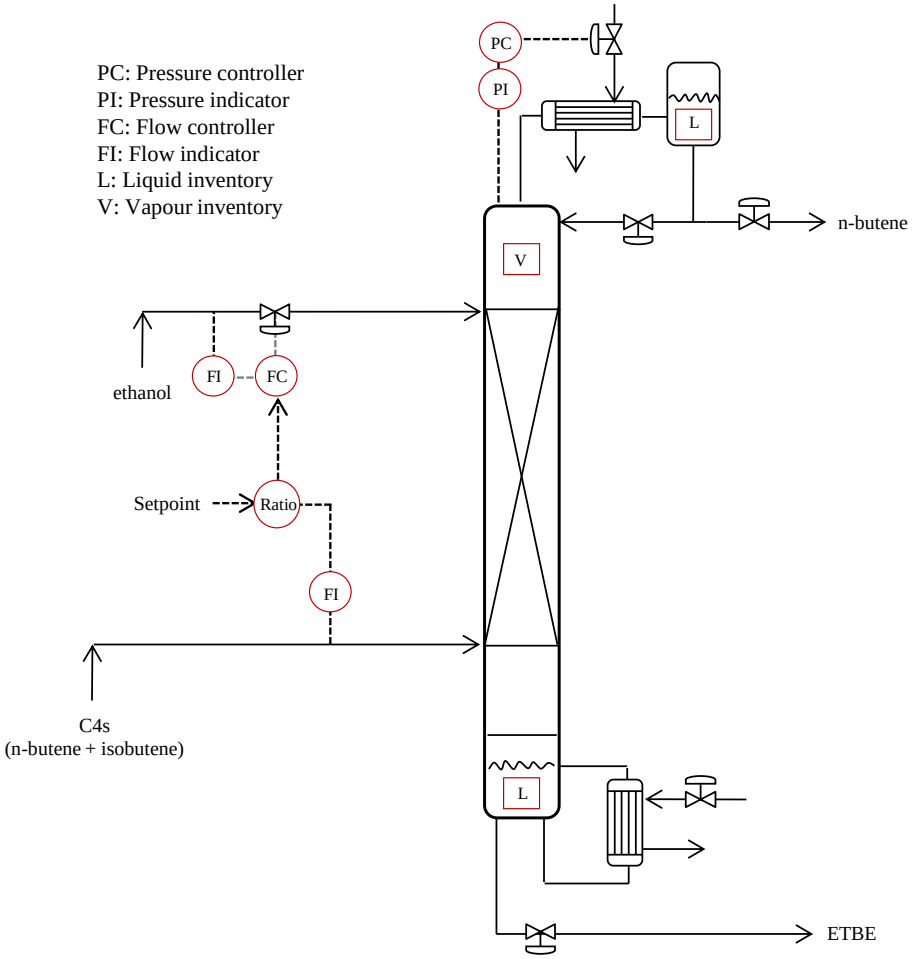

315

316 Fig. 2. Process flow diagram of ETBE reactive distillation column.

317 The reaction kinetic correlations applied in this research, are (Al-Arfaj and Luyben 2002; Zhang, et al.

318 1997):

$$r_{ETBE} = \frac{M_{cat}\, k_{rate}\, a_{ethanol}{}^{2}\, (a_{isobutene} - \frac{a_{ETBE}}{K_{ETBE}})}{(1 + K_A\, a_{ethanol})^3} \qquad (7)$$

319 in which:

$$a_i = \gamma_i\, x_i \quad , i = ETBE, ethanol, isobutene$$

$$K_{rate} = 7.418 \times 10^{12} \exp\left(\frac{-60.4 \times 10^3}{RT}\right)$$

$$K_{ETBE} = 10.387 + \frac{4060.59}{T} - 2.89055 \ln T - 0.0191544\, T + 5.28586 \times 10^{-5}\, T^2 - 5.32977 \times 10^{-8}\, T^3$$

$$\ln K_A = -1.0707 + \frac{1323.1}{T}$$

In above, a_i is the activity, γ_i is the liquid activity coefficient, x_i is the liquid mole fraction, R is the gas constant [J.mol^{-1}.K^{-1}], M_{cat} is the mass of the catalyst [g], and T is the temperature [K].

3.2. Pre-optimization analysis: reaction modeling approaches

Researchers considered two approaches for modeling ETBE reactive distillation columns. These are modeling based on kinetic correlations (applied by Luyben and Yu, 2008, Bisowarno, et al. 2003, Miranda, et al. 2008) and modeling based on the assumption of chemical equilibrium (applied by Sneesby, et al. 2000, Khaledi and Young, 2005). Since assuming chemical equilibrium implies that the residence time is large enough to maximize the conversion, it is expected that the results of this modeling approach feature a higher overall conversion. However, Luyben and Yu, (2008) (Page 236, top paragraph) reported an unexpected result when they compared the above two models:

"*the conversion dropped to less than 50%, and the concentration of the both reactants in the entire reaction zone were quite high. We are at a loss to explain these results.*"

This study took the opportunity to sort out the problem identified by these authors for the sake of completeness. Fortunately, the updated code presented in Appendix is able to provide the comparison accurately. Therefore, a contribution of this research was improving the model of ETBE reactive distillations.

In the comparison, the number of rectifying stages was 2; the number of reactive stages was 18; the number of stripping stages was 4; the ethanol feed stage was 7; the C4s feed stage was 20; the reflux ratio was 7; the column pressure was 7.5 atm and the pressure drop was 0.01 atm.tray^{-1}; the catalyst holdup of each tray was 1000 kg; the ethanol feed flow rate was 716 (kmol.h^{-1}); the bottom product flow rate was 714 (kmol.h^{-1}); the C4s feed consisted of 706.8 (kmol.h^{-1}) isobutene and 1060.2 (kmol.h^{-1}) n-butene. The calculation of the equilibrium reaction was based on minimization of Gibbs free energies. The two modeling approaches will be compared later in results Section. Notice that in the terminology of Aspen Plus®, the first stage is the condenser and the last stage is the reboiler.

3.3. Integrated design and control of an ETBE reactive distillation using a steady-state inversely controlled process model

In the subsequent subsections, the optimization constraints, the optimization variables, the goal driven objective function, the implemented software tools and treatment of the software failures are discussed.

3.3.1. Optimization constraints

Optimization constraints can be classified into the constraints regarding (1) disturbance scenarios, (2) the available degrees of freedom (3) perfect control, and (4) first principles modeling. These constraints are discussed in the following.

3.3.1.1. Constraints regarding disturbance scenarios

As discussed by Al-Arfaj and Luyben (2002), it is less likely to have control over the flow rate or composition of the C4s feed. However, the ethanol feed is delivered from storage and its flow rate can be adjusted as a manipulated variable. Therefore, the C4s feed stream is the source of disturbances. The C4s feed is a mixture of isobutene and n-butene. Luyben and Yu, (2008) considered two disturbance scenarios, 1) changes in the flow rate or 2) changes in the composition of the C4s feed. In the present case study, both these disturbances are considered simultaneously. In each disturbance scenario, the molar flow rate of each of the components in the feed stream is changed by ±10%. The combinations of these changes result in nine disturbance scenarios shown in Table 3. These disturbance scenarios are equally likely.

Table 3

Disturbance scenarios: ±10% changes in the molar flowrates of isobutene and n-butene

Disturbance Scenario	Isobutene (molar fraction) [-]	Isobutene [kmol.h^{-1}]	N-butene (molar fraction) [-]	N-butene [kmol.h^{-1}]
1st	0.9	636.12	0.9	954.18
2nd	0.9	636.12	1	1060.20
3th	0.9	636.12	1.1	1166.22
4th	1	706.80	0.9	954.180
5th	1	706.80	1	1060.20
6th	1	706.80	1.1	1166.22
7th	1.1	777.48	0.9	954.18
8th	1.1	777.48	1	1060.20
9th	1.1	777.48	1.1	1166.22

3.3.1.2. Constraints regarding the available degrees of freedom and inventory control systems

The aim of the following analysis is to establish the available degrees of freedom for the optimization framework.

Konda, et al. (2006) proposed a flowsheet-oriented method for degree of freedom analysis. They showed that the number of the degrees of freedom for a total reflux distillation column is six. Since the ETBE reactive distillation column has two feed streams, using the above method, the total degrees of freedom will be seven. However, since the C4s feed is the source of potential disturbances, it consumes one degree of freedom. The remaining six degrees of freedom are shown by the six control valves in Fig. 2.

There are three mass inventories, i.e., two liquid inventories at the column ends, in addition to the column vapor inventory. The engineering practice is to control the column pressure (representing the vapor inventory) using the cooling duty of the condenser, as shown in Fig. 2. The overhead liquid inventory can be controlled using either the reflux flow rate or the distillate flow rate, which imposes the following constraints:

$$Y_D + Y_R = 1 \qquad (8a)$$

In addition, the bottom liquid inventory can be controlled using either the reboiler duty or the bottom flowrate, which imposes another constraint:

$$Y_B + Y_{Q_H} = 1 \qquad (8b)$$

Since, in the new formulation (Problem II), no binary variable is assigned to the manipulated and controlled variables, constraints (8a,b) were implemented using an "if" procedure, which added to the penalty function when the these constraints were violated.

There is another hidden constraint which also concerns the material balances. This constraint is imposed by the reaction stoichiometry (equation 6) and requires that for one kmol of isobutene, one kmol of ethanol should be fed in order to produce one kmol of ETBE. For this reason, a ratio controller is included in Fig. 2 and the ratio of the C4s feed to ethanol feed is controlled. However, since the disturbances may include changes in the composition of the C4 feed, the setpoint of this controlled variable may need adjustment, which returns an extra degree of freedom.

In summary, there are three variables equivalent to two manipulated variables and a setpoint, which can be optimized by the optimization framework. They are (1) either the distillate flowrate or the reflux flowrate (2) either the bottom flowrate or the reboiler duty, (3) the ratio between the C4s feed and the ethanol feed.

3.3.1.3. Constraints regarding perfect control

In Section 2.1, the problem formulation was modified and the penalty functions (2a-c) were introduced. In this case study, the above constraints were implemented by the *sortrows* command of MATLAB®. In each optimization iteration, the $sortrows$ command ranked the candidate controlled and manipulated variables according to their deviation variables.

Table 4 lists the candidate controlled and manipulated variables for the case of an ETBE reactive distillation column. In this table, the notations R, D, B represent reflux, distillate, and bottom streams respectively. The notation T_i represents the temperature of the tray i and Q_H refers to the heat duty of the reboiler.

The industrial practice is to avoid online composition analyzers if possible due to their high costs, as discussed by Huang, et al. (2012). Therefore, only temperature measurements are considered for

quality control. However, the setpoints of the inferential temperature controlled variables can be employed by a secondary control layer including composition controllers. This scenario is investigated in the post-optimization analyses and using dynamic simulation, as will be discussed later.

Table 4

Candidate controlled and manipulated variables for the ETBE reactive distillation

Candidate variables to be selected as controlled variables (y_i in equation 2b)	$T_1, \dots, T_{Ntrays}$, $\frac{R}{D}, \frac{R}{B}, \frac{R}{F^{C4s}}, \frac{R}{F^{EtOH}}, \frac{D}{B}, \frac{D}{F^{C4s}}, \frac{D}{F^{EtOH}}, \frac{B}{F^{C4s}}, \frac{B}{F^{EtOH}}$
Candidate variables to be selected as manipulated variables (u_j in equation 2c)	R, D, B, Q_H

3.3.1.4. Constraints regarding first principles modeling

The first principles modeling was perform using Aspen Plus® and according to the guidelines by Luyben and Yu (2008). The components were defined from the software databank. The UNIFAC property method was used for liquid phase analysis and the Peng-Robinson property method was applied for vapor phase analysis. The Radfrac distillation model with total reflux was used and the option for the solver was set to *strongly non-ideal liquid*. The underlying equations of these models (i.e., Radfrac, Peng-Robinson, UNIFAC) can be found in Aspen Plus® documents (2008a,b). As mentioned earlier, one modeling approach is to assume chemical equilibrium. However, as will be shown later, this assumption may overestimate the actual reaction conversion. In this research, the reaction kinetic correlations (equation 7) are applied for modeling. Since these correlations include activity terms, it is not possible to use the Aspen Plus® reaction forms, and the kinetic correlations were introduced to the software using a Fortran subroutine. Luyben and Yu, (2008) provided the original Fortran subroutine. Unfortunately, due to the changes in the way that Aspen Plus® uses the memory, that code is outdated for Aspen Plus® 2006 and later versions. The updated subroutine, based on a solution (121621) by AspenTech® support website, is provided in the appendix.

3.3.2. Optimization variables

Optimization variables are listed in Table 5. They can be classified into 1) process parametric variables, 2) process structural variables, 3) control parametric variables, and 4) control structural variables. The numbers of the stages in each distillation section and the trays of the feeds are the process structural variables. The amount of the catalysts on each tray and the column pressure are the process parametric variables. The amount of the catalysts on each tray however, is bounded by the tray diameter, and was checked in each optimization iteration using the built-in tray sizing function of Aspen Plus®. As will be discussed later, due to difficulties with convergence of the simulation solver, two new sets of optimization variables were introduced. They were $\alpha_{1,s}$ which represents the molar ratio of the bottom product flow rate to the ethanol feed flow rate, and $\alpha_{2,s}$ which represents the molar ratio of the ethanol feed flow rate to the isobutene flow rate in the C4s feed. Therefore, the control parametric variables are reflux ratios, $\alpha_{1,s}$ and $\alpha_{2,s}$. The structural variables for selection of controlled and manipulated variables are not shown in Table 5. They are implied in the penalty functions 2a-c. By convergence of the optimization algorithm, the values of two terms ($DOF = 2$, equal to the number of steady-state degrees of freedom) in this penalty function will be zero. These two terms correspond to two variables in Table 4 and determine which two candidate controlled or manipulated variables are selected. In an intermediate stage of the optimization procedure, while the process structural and parametric variables and control structural variables have the same values for all disturbances, the required values of the control parametric variables (Reflux ratio_s, $\alpha_{1,s}$ and $\alpha_{2,s}$), vary according to different disturbance scenarios and therefore are identified by the corresponding index $s = 1, \dots, 9$ in Table 5.

Table 5

Optimization variables; $\alpha_{1,s}$ represents the ratio $F_s^{bottom}/F_s^{Ethanol-Feed}$ for disturbance scenario s. $\alpha_{2,s}$ represents the ratio $F_s^{Ethanol-feed}/F_s^{isobutene-Feed}$ for disturbance scenario s.

Optimization variables	**Description**	**Optimization variables**	**Description**
Number of rectifying trays	Process structural variable	Reflux ratio$_{s=2}$	Control parametric variable
Number of reactive stages	Process structural variable	Reflux ratio$_{s=3}$	Control parametric variable
Number of stripping stages	Process structural variable	Reflux ratio$_{s=4}$	Control parametric variable
ethanol feed stages	Process structural variable	Reflux ratio$_{s=5}$	Control parametric variable
C4s feed stages	Process structural variable	Reflux ratio$_{s=6}$	Control parametric variable
Column Pressure [atm]	Process parametric variable	Reflux ratio$_{s=7}$	Control parametric variable
Catalyst hold-up [kg]	Process parametric variable	Reflux ratio$_{s=8}$	Control parametric variable
$\alpha_{1,s=1}$	Control parametric variable	Reflux ratio$_{s=9}$	Control parametric variable
$\alpha_{1,s=2}$	Control parametric variable	$\alpha_{2,s=1}$	Control parametric variable
$\alpha_{1,s=3}$	Control parametric variable	$\alpha_{2,s=2}$	Control parametric variable
$\alpha_{1,s=4}$	Control parametric variable	$\alpha_{2,s=3}$	Control parametric variable
$\alpha_{1,s=5}$	Control parametric variable	$\alpha_{2,s=4}$	Control parametric variable
$\alpha_{1,s=6}$	Control parametric variable	$\alpha_{2,s=5}$	Control parametric variable
$\alpha_{1,s=7}$	Control parametric variable	$\alpha_{2,s=6}$	Control parametric variable
$\alpha_{1,s=8}$	Control parametric variable	$\alpha_{2,s=7}$	Control parametric variable
$\alpha_{1,s=9}$	Control parametric variable	$\alpha_{2,s=8}$	Control parametric variable
Reflux ratio$_{s=1}$	Control parametric variable	$\alpha_{2,s=9}$	Control parametric variable

3.3.3. Instances of the goal-driven objectives and their target values

This section presents the instances of the objective functions in Table 1 for the case of an ETBE reactive distillation column. The instances of the first objective are the purity of the ETBE (bottom) product stream (99% mass fraction of ETBE) and the purity of the overhead product stream (less than 2% mass fraction of isobutene). The purity of the overhead product is defined as an inequality so the optimizer will find the optimal conversion extent by maximizing the ETBE production against costs.

There are six manipulated variables in the ETBE reactive distillation, as shown in Fig. 2. Since in this case study, disturbances include the changes in the feed flow rate, three of these manipulated variables (i.e., the ethanol feed, the overhead product and the bottom product) must change according to the reaction stoichiometry; therefor, their changes are necessary for perfect control and are not penalized. The variations of the remaining manipulated variables, (i.e., the reboiler and condenser duties and the reflux flow rate) are the instances of the second objective function.

The variations in the composition of all four components (i.e., isobutene, n-butene, ethanol, and ETBE) all through the column are the instances of the third objective.

As mentioned earlier, a target value is needed for the fourth (economic) objective. Total Annual Profit (TAP) is:

$$\mathrm{TotalAnnualProfit} = \mathrm{Total\ AnnualRevenue} - \mathrm{TotalAnnualCosts} \quad (9a)$$

$$\mathrm{TotalAnnualCosts} = \mathrm{Capitalcosts/paybackperiod} + \mathrm{annual\ energy\ costs} + \mathrm{annualfeedstockcosts} \quad (9b)$$

Generating an optimistic target value for the fourth objective is straightforward. This can be done by ignoring Total Annual Costs, and calculating the Total Annual Revenue which is simply the revenue from the products minus the costs of the raw materials, and only requires mass balance information. The results of this analysis showed that $TAP^{max}=2.9\times10^{8}$ \$.yr^{-1}.

The values of the weighting factors of the goal programming objective function (4) were selected to be $w_1 = 100$, $w_2 = 1$, $w_3 = 0.1$, $w_4 = 10$. For these choices of the weighting factors, all the terms in the multi-objective function have the same order of magnitude.

Table 6

Economic data for calculating Total Annual Profit (Equations 9a and b)

	Economic parameters	Reference
C4s Feed [\$.kmol^{-1}]	29.65	ICIS pricing (2011)
ethanol [\$.kmol^{-1}]	39.67	ICIS pricing (2011)
ETBE [\$.kmol^{-1}]	118.25	ICIS pricing (2011)
Amberlyst 15 (Catalyst) [\$.kg^{-1}]	10.16	Al-Arfaj and Luyben (2002)
Low Pressure (LP) Steam[\$.kg^{-1}] (P=9.4 bar, T=451.7 K)	0.0019	Ulrich and Vasudevan (2006)
Cooling Water [\$.kg^{-1}] (P=7 bar, Tsupply=30 ^{o}C)	0.0414	Ulrich and Vasudevan (2006)
	Sizing correlations and parameters	Reference
Capital costs of heat exchangers [\$] ($Area$ =[m^2])	$7296 Area^{0.65}$	Al-Arfaj and Luyben (2002)
Heat transfer coefficient (condenser) [kW.K^{-1}m^{-2}]	0.852	Al-Arfaj and Luyben (2002)
Heat transfer coefficient (reboiler) [kW.K^{-1}m^{-2}]	0.568	Al-Arfaj and Luyben (2002)
Capital cost of column Vessel (D =[m]; L =[m])	$17640 D^{1.066} L^{0.802}$	Al-Arfaj and Luyben (2002)
Payback period [years]	3	Al-Arfaj and Luyben (2002)

Table 6 lists the economic parameters and the sizing correlations used in this case study. Required information for the prices of the products, utilities and feedstocks were from Al-Arfaj and Luyben (2002), ICIS pricing (2011) and Ulrich and Vasudevan (2006). The reference year was 2010, and the prices from Al-Arfaj and Luyben (2002) and Ulrich and Vasudevan (2006) were updated using Chemical Engineering Plant Cost Index (CE PCI) and Marshall & Swift Equipment Cost Index (M&S ECI) from Chemical Engineering, (2011). Different disturbances require different operating and capital costs. Since the disturbances are assumed equally likely, the average of the operating costs are considered. However, because equipment should remain operable for all disturbance scenarios, the highest capital costs are considered.

3.3.4. Implementation software tools

Simulation-optimization programming was applied in this research, which is proved efficient for incorporating process simulators into optimization frameworks (Caballero, et al. 2007; Sharifzadeh, et al. 2011). Here, the simulation program acts as the implicit constraints and is solved in the inner loop. The simulation provides the values of the objective functions and the penalty function and has a black-box input-output relationship to the optimizer which is solved in the outer loop. In the present case study, simulation was performed using Aspen Plus® and optimization was performed by Genetic Algorithm (GA) Toolbox of MATLAB®. Unfortunately, due to technical difficulties it was not possible to link MATLAB® directly to Aspen-Plus®. Therefore, MATLAB® was firstly linked to Microsoft Excel/VBA® and then Microsoft Excel/VBA ® was linked to Aspen Plus®. Integration was based on Microsoft COM® automation interface. The default settings were applied for generic algorithm. The details of optimization software can be found in MATLAB® documentation, (2012).

Fig. 3 shows the information flow of simulation-optimization program. The left-hand side block and the right-hand side block are GA Toolbox® and Aspen Plus® simulator respectively. The middle block comprises of an m.file coded in MATLAB® and a Microsoft Excel/VBA® code, which integrate the two software tools. Note that due to formulation of the penalty function, it is not needed anymore to construct the inverse model in each optimization iteration.

The steps in each optimization iteration are as follows:

Step 1. The GA decides on the values of the optimization variables, (Table 5).

Step 2. The integrating code receives the values of the optimization variables, and set them in the simulation program.

Step 3. The disturbances are imposed by changing the flow rate and the composition of the C4s feed as described earlier.

Step 4. For each disturbance scenario, the corresponding values of the objective functions (Table 1) are evaluated. Then, the aggregated value of the multi-objective function (4) is constructed and penalized by the penalty functions (2) and then reported to the GA.

Step 5. The GA evaluates the termination criteria and decides on improving the optimization variables.

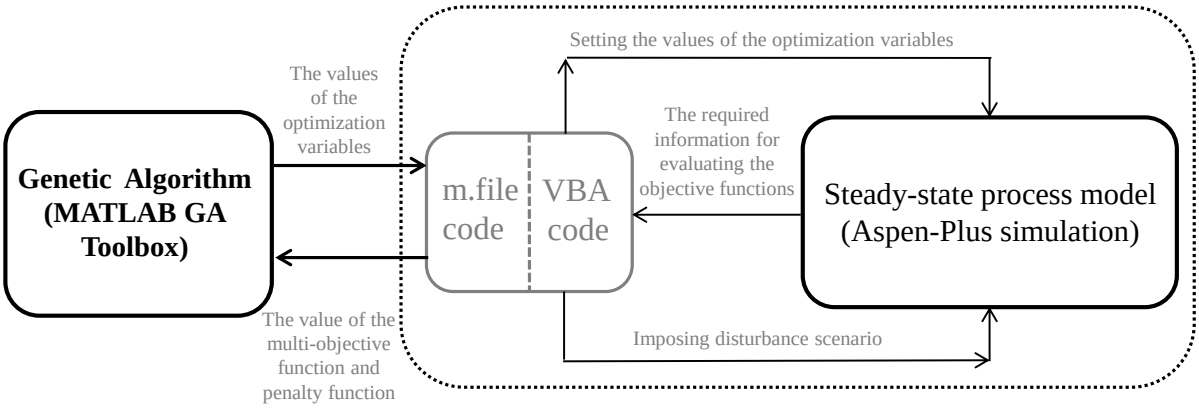

Fig. 3. Information flow of the simulation-optimization programming.

In each simulation run, a simulation file was opened, run, and closed without saving. Since nine disturbance scenarios were considered, for each function recall (i.e., one evaluation of the objective function) the simulation was run nine times. The required time for each function recall was 4-5 minutes, which in the problematic cases when the solver had problems with convergence was significantly more. Each generation of the optimization algorithm had twenty individuals, and the optimization needed up to fifty generations. Therefore, each optimization run needed up to one week before a reasonable solution can be achieved. In addition, in order to refine the

529 penalty functions and weighting factors of the objectives, the optimization procedure needed to
530 be interrupted and/or reiterated a few times.

531 *3.3.5. Treatment of divergence of the equation solver*

532 As explained earlier in Section 2.1, the advantage of including the penalty functions (2a-c) is that
533 there is no need to construct an inversely controlled process model in each iteration of the
534 optimization procedure. Therefore, this formulation provides the opportunity to choose those
535 simulation specifications which are more likely to ensure convergence of the simulation program, as
536 discussed in the following.

537 The author encountered difficulties in simulation-optimization of the case study as the simulation was
538 frequently diverging. Divergence of the simulator solver was also reported by Luyben and Yu (2008),
539 when they were investigating the effects of the design parameters:

540 *"Convergence issues and frequent Fortran system errors severely limited this investigation."*

541 In the present study, the author's observations suggested that there were two types of solver
542 divergence. Firstly, since the solver is principally a nonlinear equation solver, its success depends on a
543 close starting point. Strategies such as setting the solver for the maximum possible iterations, or
544 automated re-initialization of the solver greatly improved this type of divergence. However, the
545 second type of divergence could be due to infeasible trial values for the optimization variables.
546 Unfortunately, solver divergence is not informative and the solver does not inform the optimizer about
547 the degree and cause of infeasibility. One resolution is to cruelly penalize the objective function. The
548 risk is that the optimizer may converge to an easy local optimum. In this study, two instances for the
549 second type of divergence were identified and resolved. The first instance was due to a reflux value
550 that was not appropriate to remove products and introduce fresh feeds to the reactive trays. In that
551 instance, reflux was changed by +25%, -25%, and +50%. At the same time, a penalty value was added
552 to the objective function. This strategy ensures that the value of the objective function reflected some
553 fitness of the problematic solution, while the ultimate solution was feasible and converging.

554 The second instance of solver failure was due to inconsistency with the reaction stoichiometry.
555 Equation 6 suggests that for a kmol of isobutene in the feed, only a kmol of ethanol participates in the

reaction and any extra ethanol would degrade the purity of the ETBE product. This analysis suggests that the value of $\alpha_{1,s}$ and $\alpha_{2,s}$ (in equations 10a, b below) should be tightly bounded around unity in order to maintain molar balance of the column:

$$F_s^{bottom} = \alpha_{1,s} \times F_s^{ethanol\ feed} \quad (10a)$$

$$F_s^{ethanol\ feed} = \alpha_{2,s} \times F_s^{isobutene\ Feed} \quad (10b)$$

$$0.95 < \alpha_{i,s} < 1.05, \qquad i = 1,2 \quad (10c)$$

where $F_s^{isobutene\ Feed}$ is molar flow rate of isobutene in the C4s feed for disturbance s, $F_s^{ethanl-feed}$ is the molar flow rate of the ethanol feed for disturbance s, F_s^{bottom} is the molar flow rate of the bottom product for disturbance s. In this research, the above constraints were added to the simulation-optimization framework. $F_s^{ethanl-feed}$ and F_s^{bottom}, were selected as the simulation specifications, and their values were calculated using the trial values of $\alpha_{1,s}$ and $\alpha_{2,s}$ from the optimization algorithm. This strategy ensured that eighteen optimization variables in Table 5 are almost near their optimal values and the solver would not diverge due to inconsistency with the reaction stoichiometry. In the present study, the application of the abovementioned strategies brought all simulations into convergence. In each iteration of the inner-loop simulation, the status of the solver was checked and the objective functions were only evaluated after simulation convergence.

3.4. Post-optimization controller design

It was explained earlier, that the results of the applied optimization framework based on perfect control can be used by the control practitioners for actual controller design. In this research, post-optimization analyses were conducted, in which actual PI controllers were designed for the optimized process and its control structure (i.e., the results of the optimization framework). Two sets of post-optimization analyses were performed. In the first set, the control structure did not include the composition analyzer for the product purity and they were controlled inferentially by controlling the temperature of two trays. In the second set, a secondary composition controller layer decided the setpoints of the temperature controllers. The aim was to investigate the importance of composition controllers. The considered disturbance scenarios for these analyses included ±10% and ±20% changes in the C4s feed flowrate. Notice that the ±20% disturbance scenarios were far beyond the considered disturbance scenarios (Table 3) in the optimization framework. The aim was to investigate the sensitivity of the solution to unforeseen disturbances. The applied procedures for converting the steady-state simulation to the dynamic simulation and tuning controllers can be found in Luyben, (2006).

It is important to remember that the aforementioned post-optimization studies using decentralized PI controllers is for demonstration only and the applied optimization framework does not make any presumption regarding the type of controllers. Therefore, the optimized process and its control structure can be implemented using other controllers (e.g., MPCs) as well.

4. Results and discussions

The results and discussions are presented in three parts. Firstly, the results of pre-optimization analysis is presented and discussed. The aim of that part of research is to justify the choice of the reaction modeling approach. Then the results of the reformulated optimization framework is presented and discussed and finally in the post-optimization analysis, actual controllers are designed for the optimized process and control structure.

4.1. Pre-optimization results and discussions

Figs. 4a-e provide the opportunity for comparisons between modeling based on the kinetic correlations and modeling based on chemical equilibrium. It is expected that the overall conversion will be higher for the chemical equilibrium assumption, because in this case it is assumed that the residence times are large enough that the reaction conversions are maximized. Figs. 4b to e show that this expectation is true, and for the same operating conditions, the purity of the products at the column ends are about 3% higher for the model based on chemical equilibrium. Since the reaction is exothermic and the model based on chemical equilibrium predicts high conversions, the temperature profile of this model is also higher than the temperature profile of the model based on the kinetic correlations, as shown in Fig. 4a. In the modeling based on chemical equilibrium, it is assumed that the residence times on the reactive trays are large enough, so the reaction conversions approach the equilibrium extents. Large residence times imply small flowrates or large liquid hold-ups on the reactive trays. Therefore, if the actual liquid hold-ups and flowrates do not meet the requirements for large residence times, the reactants may leave the reactive trays unconverted and as a result, the designed process may not be able to meet the product specifications. Therefore, in the present case study, the kinetic modeling approach was selected conservatively.

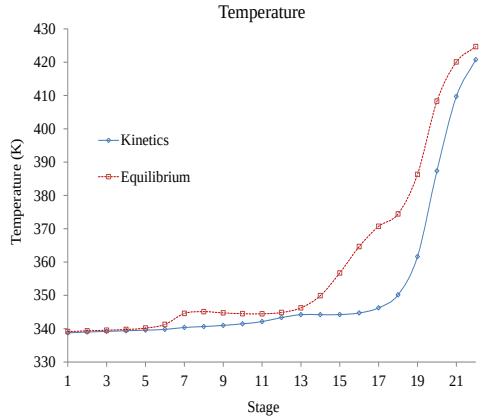

Fig. 4a. The temperature profiles calculated based on the kinetic correlations (blue circles) and the equilibrium reaction assumption (red squares).

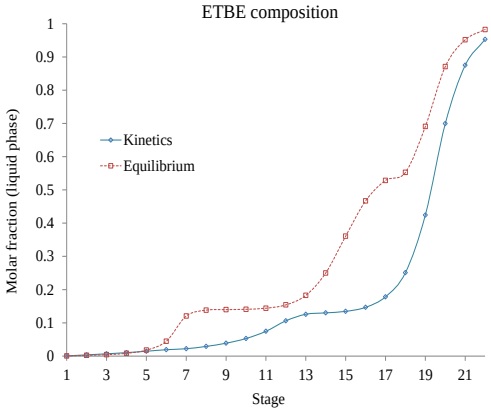

Fig. 4b. The composition profiles of ETBE calculated based on the kinetic correlations (blue circles) and the equilibrium reaction assumption (red squares).

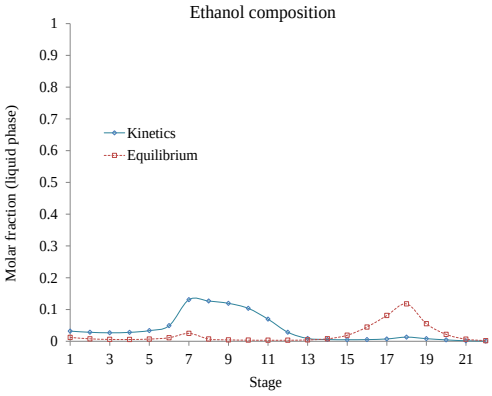

Fig. 4c. The composition profiles of ethanol calculated based on the kinetic correlations (blue circles) and the equilibrium reaction assumption (red squares).

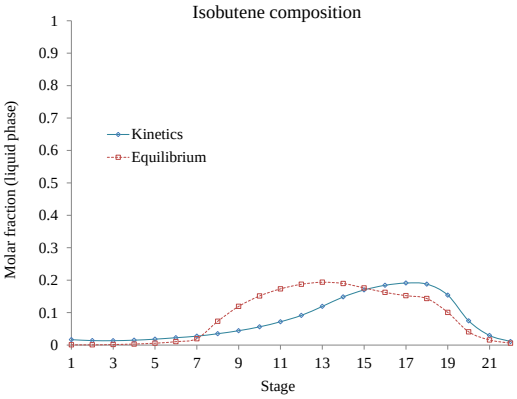

Fig. 4d. The composition profiles of isobutene calculated based on the kinetic correlations (blue circles) and the equilibrium reaction assumption (red squares).

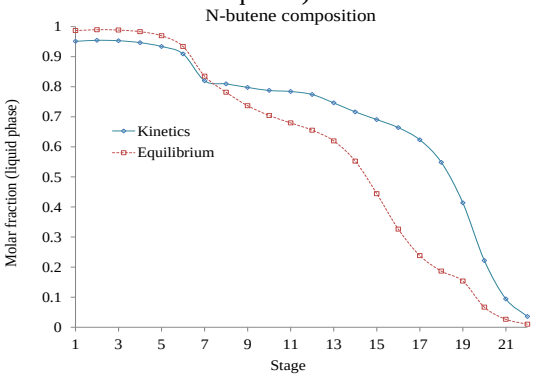

Fig. 4e. The composition profiles of n-butene calculated based on the kinetic correlations (blue circles) and the equilibrium reaction assumption (red squares).

4.2. Integrated design and control: results and discussions

Table 7 reports the optimal values of the objective functions. The value of the first objective suggests that the product quality is successfully controlled in the presence of the disturbances in the flowrate and composition of the C4s feed. The value of the second objective concerns the changes in the manipulated variables. While adjusting the manipulated variables is necessary for rejecting the disturbances, excessive changes in the manipulated variables are undesirable, because they may invoke interactions between the control loops and increase maintenance costs, (McAvoy, et al, 2003). The average value of 4.37% changes in the manipulated variables suggests that the excessive changes in the manipulated variables are suppressed. In addition, although the value of 13.5% is reported for the variations of the internal states, as shown in Fig. 5c, most of these variations are related to ethanol and are limited to the area of the C4s feed entrance where disturbances were imposed to the column. The rest of the process remains controlled tightly. Finally, comparing the value of the economic objective function to the target value of 2.9×10^{8} suggests that the losses associated with disturbances are limited to only 1.24%.

Table 7

The values of the objective functions

Average purity of the ETBE product (mass fraction) [-]	Average changes in manipulated variables	Average changes in intermediate compositions	Average Total Annual Profit (TAP) [$.yr^{-1}]
0.9866	4.37%	13.52%	2.864×10^{8}

Fig. 6a presents the optimized process and control structure. In a double-feed reactive distillation, the common practice is to feed the heavy (i.e., ethanol) and the light reactants (i.e., isobutene) above and below the reactive section respectively (e.g., Fig. 2). Then, as the heavy reactant travels to the bottom and the light reactant travels to the top, they react and are converted to the products. However, in the optimized process, the optimizer chose to expand the reactive section and to feed the heavy reactant in the middle of the reactive section. Therefore, the reactive trays above the heavy reactant entrance are responsible for both separation and reaction and these two phenomena are highly integrated. In

addition, the optimizer chose to feed the C4s in the stripping section. As a result, the light components (isobutene and n-butene) carry the heavy unreacted component (ethanol) back to the reactive section. As shown in Table 8, the optimizer also chose high reflux ratios. This decision implies increasing the liquid hold-ups in the overhead and bottom accumulators and on the trays. Therefore, the optimized design is less sensitive to disturbances.

Figs. 5b-e show that the control structure was successful in tightly controlling the compositions of the components. The variations in the profiles are limited to the entrance area of the C4s feed, where the changes in the feed flowrate and composition cause the variations. However, the compositions are tightly controlled at the column ends.

The selected control structure includes controlling the temperature of the first tray and the temperature of the twelfth tray. Figs. 6a and b illustrate the selected controlled variables and the required controlled variables for controlling material inventories implemented in multi-loop control structures. The regulatory control structures are the same in the both figures. However, the control structure in Fig 6b has a supervisory control layer using composition controllers. These control structures are further studied in the next section, using dynamic simulation.

It is also notable that in conventional distillation columns, when the reflux ratio is larger than three, the reflux flowrate is used for controlling the liquid inventory of the overhead accumulator, because it has a larger gain. In that scenario, the distillate flowrate would be left for controlling the temperature of the first tray. However, the author's observation was that designing such a control structure for the ETBE reactive distillation column results in an interacting and oscillating control scheme. The reason is that in a reactive distillation column, the reflux directly affects the rate of the reactions by returning unreacted materials to the trays. As a result, controlling the overhead inventory using reflux influences the reaction rates which in turn perturb the composition and temperature profiles of the column. Therefore, in the present case study, the distillate is used for controlling the overhead liquid inventory and the controlled variable corresponding to the temperature of the first tray is paired with the reflux. With similar justification, the controlled variable corresponding to the temperature of the

twelfth tray is paired with the reboiler duty and the liquid inventory of the bottom accumulator is controlled using the flowrate of the bottom product.

Table 8

Optimal values of the optimization variables.

Optimization variables	**Optimal value**	**Optimization variables**	**Optimal value**
Number of rectifying stages*	2	Reflux ratio$_{s=1}$ [-]	6.88
Number of reactive stages	16	Reflux ratio$_{s=2}$ [-]	6.23
Number of stripping stages	4	Reflux ratio$_{s=3}$ [-]	6.35
ethanol feed stage	7	Reflux ratio$_{s=4}$ [-]	6.12
C4s feed stage	20	Reflux ratio$_{s=5}$ [-]	6.23
Column Pressure [atm]	6.44	Reflux ratio$_{s=6}$ [-]	5.75
Catalyst hold-up [kg]	1078.5	Reflux ratio$_{s=7}$ [-]	6.51
		Reflux ratio$_{s=8}$ [-]	6.51
		Reflux ratio$_{s=9}$ [-]	6.56
$F_{s=1}^{bottom}$ [kmol.h^{-1}]	626.81	$F_{s=1}^{ethanol\ feed}$ [kmol.h^{-1}]	640.56
$F_{s=2}^{bottom}$ [kmol.h^{-1}]	627.74	$F_{s=2}^{ethanol\ feed}$ [kmol.h^{-1}]	638.89
$F_{s=3}^{bottom}$ [kmol.h^{-1}]	618.02	$F_{s=3}^{ethanol\ feed}$ [kmol.h^{-1}]	628.79
$F_{s=4}^{bottom}$ [kmol.h^{-1}]	703.20	$F_{s=4}^{ethanol\ feed}$ [kmol.h^{-1}]	717.56
$F_{s=5}^{bottom}$ [kmol.h^{-1}]	697.86	$F_{s=5}^{ethanol\ feed}$ [kmol.h^{-1}]	712.14
$F_{s=6}^{bottom}$ [kmol.h^{-1}]	693.44	$F_{s=6}^{ethanol\ feed}$ [kmol.h^{-1}]	706.78
$F_{s=7}^{bottom}$ [kmol.h^{-1}]	776.78	$F_{s=7}^{ethanol\ feed}$ [kmol.h^{-1}]	787.83
$F_{s=8}^{bottom}$ [kmol.h^{-1}]	765.24	$F_{s=8}^{ethanol\ feed}$ [kmol.h^{-1}]	780.91
$F_{s=9}^{bottom}$ [kmol.h^{-1}]	755.13	$F_{s=9}^{ethanol\ feed}$ [kmol.h^{-1}]	771.18
Controlled variable (1)	Tray 1 temperature	Setpoint (1) [K]	332.8
Controlled variable (2)	Tray 12 temperature	Setpoint (2) [K]	335.6

* In this paper, the first stage refers to the condenser, and the last stage refers to the reboiler. For example, tray 12 refers to the thirteenth stage.

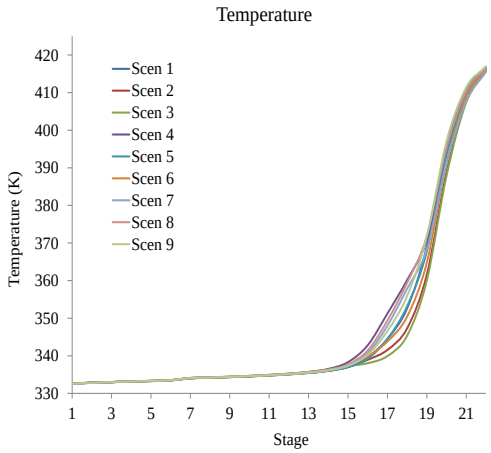

Fig. 5a. Temperature profiles of the ETBE reactive distillation column for nine disturbance scenarios.

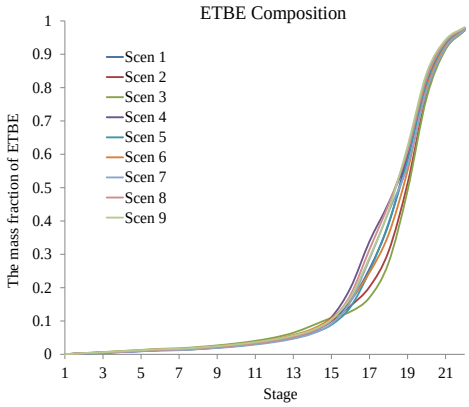

Fig. 5b. ETBE composition profiles of the ETBE reactive distillation column for nine disturbance scenarios.

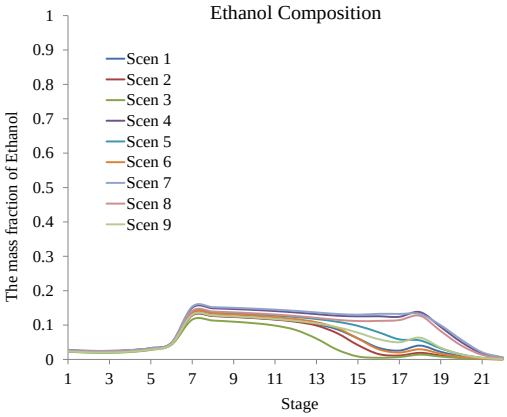

Fig. *5c*. Ethanol composition profiles of the ETBE reactive distillation column for nine disturbance scenarios.

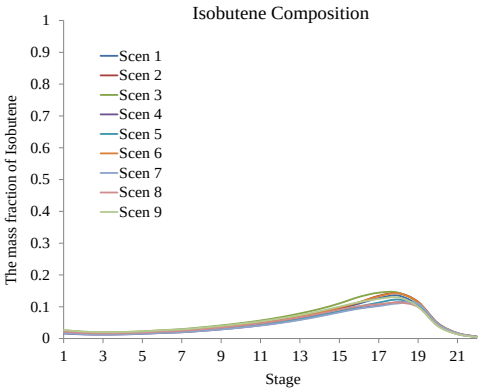

Fig. 5d. Isobutene composition profiles of the ETBE reactive distillation column for nine disturbance scenarios.

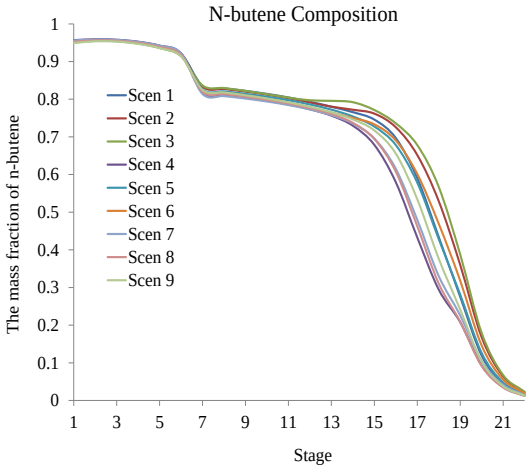

Fig. 5e. N-butene composition profiles of the ETBE reactive distillation column for nine disturbance scenarios.

671

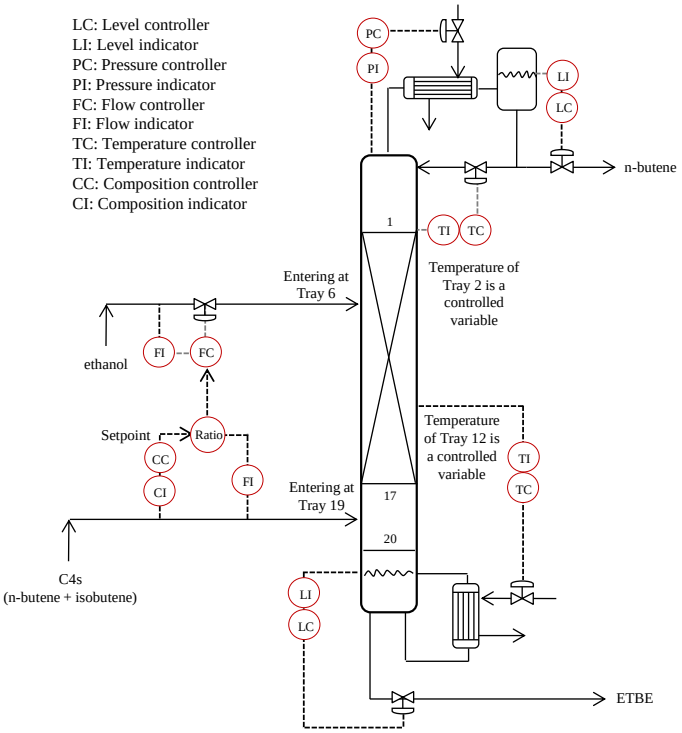

Fig. 6a. The first control structure (CS1), consisting of the inferential temperature controllers

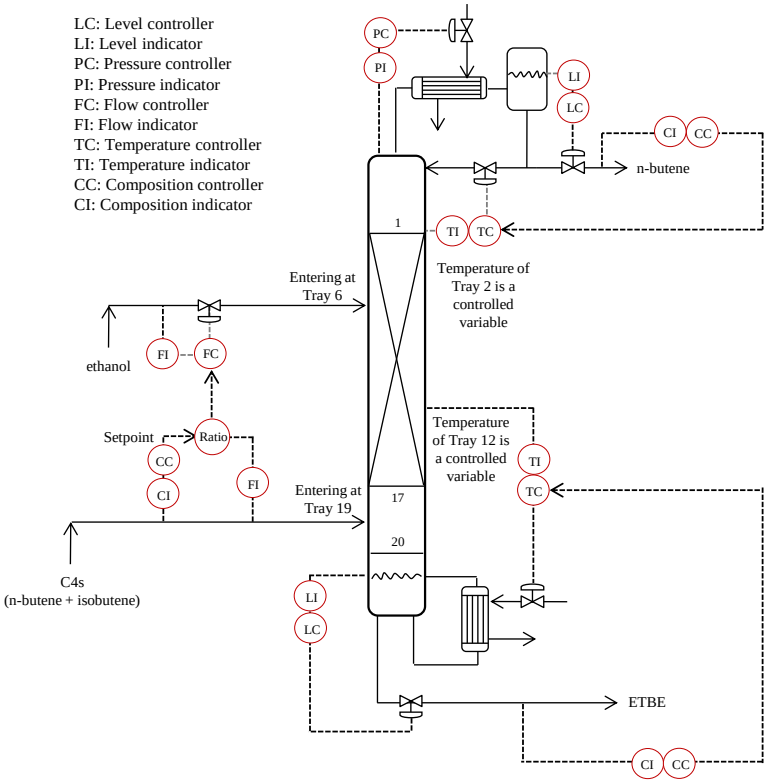

Fig. 6b. The second control structure (CS2), including the composition controllers

672

4.3. Post-optimization results and discussions

The results of the post-optimization studies are shown in Figs. 7a-h. These figures illustrate that for all disturbances, the both control structures of Figs. 6a, and b maintain the stability of the system. The worst disturbances was the +20% changes in the C4 feed which is twice larger than the disturbances for which integrated design and control was performed. Even for such a difficult disturbance the purity of the ETBE product remains above 85%, as shown in Fig. 7a. A great improvement can be made by including the secondary composition controllers as can be seen by comparing Figs. 7a and e. In Fig. 7a, the product compositions are controlled indirectly and their deviations from their desired values (i.e., composition control errors) are inferred from the deviations of the temperature controlled variables from their setpoints (i.e., temperature control errors). However, the composition control errors are highly nonlinear functions of temperature control errors. Therefore, it took five days for the system in Fig. 7a to achieve the steady-state. However, in the system of Fig. 7e, in which the compositions are directly controlled, it took only a few hours to achieve the desirable steady state. A minor drift (i.e., 0.5% mass fraction over four days) is observed for the first control structure which only employs temperature controllers. Such a drift need be remedied by the operators interventions or a secondary composition control layer, as shown in Figs. 7e-h.

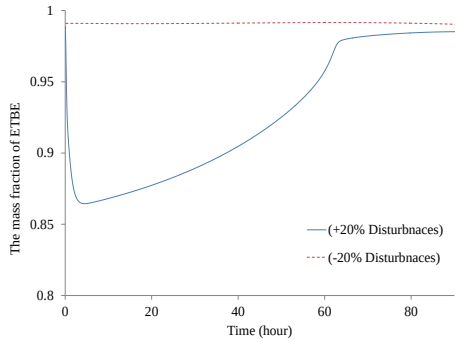

Fig. 7a. the mass fraction of the ETBE component in the bottom product, for the ±20% disturbance scenarios in the first control structure.

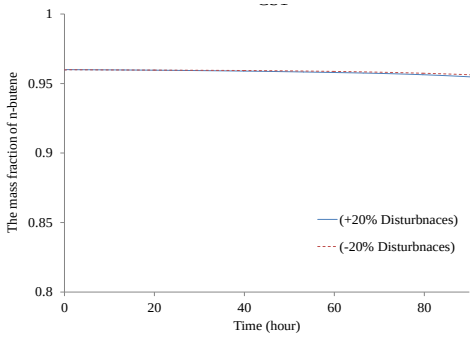

Fig. 7b. the mass fraction of the n-butene component in the overhead product, for the ±20% disturbance scenarios in the first control structure.

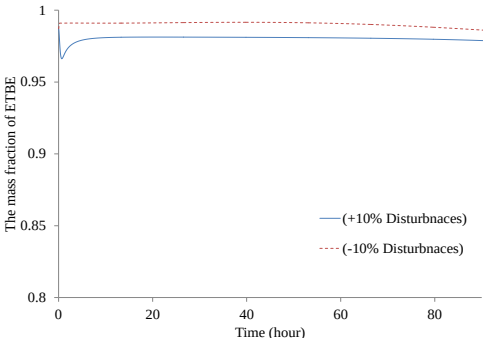

Fig. 7c. the mass fraction of the ETBE component in the bottom product, for the ±10% disturbance scenarios in the first control structure.

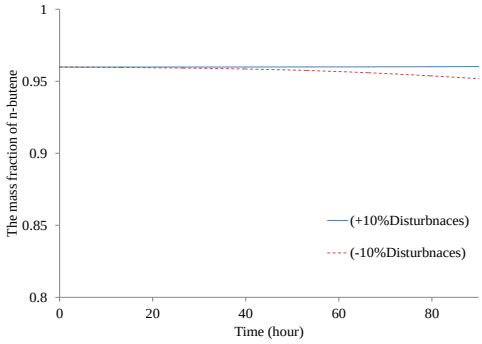

Fig. 7d. the mass fraction of the n-butene component in the overhead product, for the ±10% disturbance scenarios in the first control structure.

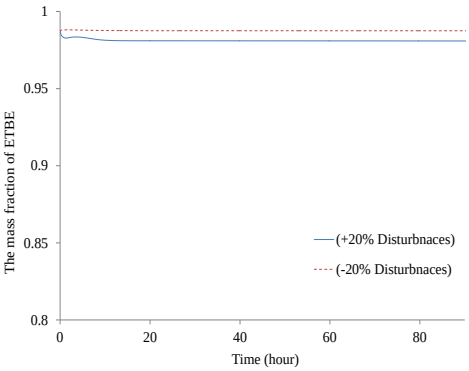

Fig. 7e. the mass fraction of the ETBE component in the bottom product, for the ±20% disturbance scenarios in the second control structure.

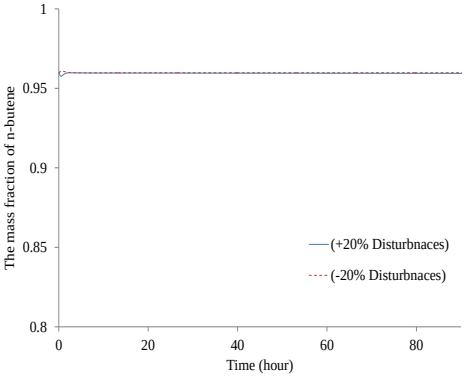

Fig. 7f. the mass fraction of the n-butene component in the overhead product, for the ±20% disturbance scenarios in the second control structure.

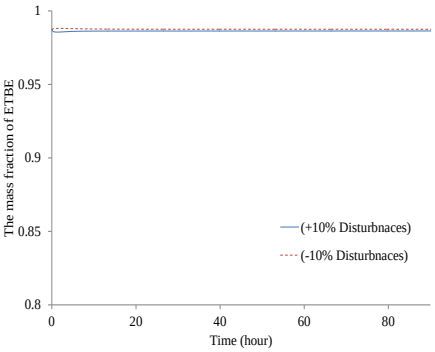

Fig. 7g. the mass fraction of ETBE component in the bottom product, for the ±10% disturbance scenarios in the second control structure.

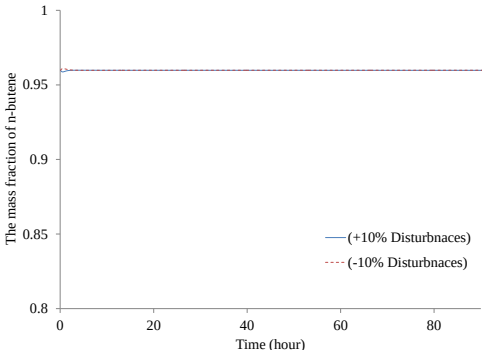

Fig. 7h. the mass fraction of n-butene component in the overhead product, for the ±10% disturbance scenarios in the second control structure.

5. Conclusion

Sharifzadeh and Thornhill (2012) introduced a steady-state optimization framework based on perfect control. This framework contributed to the aim of complexity reduction from the problem of control structure selection by separating controller design from the problem formulation. However, the process and its control structure are still optimized simultaneously, and the regulatory steady-state operability of the solution is ensured. The present paper modified and implemented that framework for steady-state integrated design and control. The modification was based on a penalty function, which ensures process model inversion, and hence perfect control. The benefits of the new formulation include less optimization variables and better convergence of the simulation program. The optimization framework was implemented for the case of an ETBE reactive distillation column. The instances of the process and control objectives for this case study were explained and their target values were justified. The applied solving strategy was based on simulation-optimization. The optimization variables were presented and the optimization constraints were discussed. The insights about the reaction stoichiometry were applied in order to further improve the convergence of the simulator solver. The implementation software tools were also explained.

The results of the integrated design and control framework demonstrated that this framework was successful to establish a trade-off between the process and control objectives. The optimized solution addressed the disturbances efficiently while the economic losses were minimized. Finally, in the post-optimization section, a decentralized PI control structure was designed for the optimized process and its control structure. The results of the post-optimization analyses suggested that even inferential temperature controller can fairly stabilize the process. Further improvement can be achieved by including a secondary composition layer. Finally, the results showed that the optimal solution was not too sensitive, and remained operable for even twice-larger disturbances.

Acknowledgement

The author gratefully acknowledges financial support from the 2010 and 2011 ISA Educational Foundation scholarships, the Burkett Scholarship and Ure bursary award of Chemical Engineering Department, Imperial College London.

References

Al-Arfaj, M.A, Luyben, W.L., 2002. Control study of ethyl tert-butyl ether reactive distillation. Industrial Engineering and Chemistry Research 41 (16) 3784-3796.

Al-Arfaj M.A., Luyben W.L., 2004. Plantwide control for TAME production using reactive distillation. AIChE Journal 50 (7) 1462–1473.

Aspen-Plus document, 2008a. Operation guide. Aspen Technology, (V7.1).

Aspen-Plus document, 2008b. Physical property methods. Aspen Technology, (V7.1).

Avami, A., Marquardt, W., Saboohi, Y., Kraemer, K., 2012. Shortcut design of reactive distillation columns. *Chemical Engineering Science*, 71, 166–177.

Babu, K.S., Kumar, M.V.P., Kaistha, N., 2009. Controllable optimized designs of an ideal reactive distillation system using genetic algorithm. *Chemical Engineering Scienc*,64, (23), 4929–4942.

Barbosa, D., Doherty, M.F., 1988. Design and minimum-reflux calculations for single-feed multicomponent reactive distillation columns. Chemical Engineering Science 43 (7) 1523-1537.

Bisowarno, B.H., Tian, Y.C., Tade, M.O., 2003. Model gain scheduling control of an ethyl tert-butyl ether reactive distillation column. Industrial & Engineering Chemistry Research 42 (15) 3584–3591.

Bogle, I.D.L., Ma K., Hagemann, J., Fraga E.S., 2004. Analysing the controllability of nonlinear process systems. In The Integration of Process Design and Control. Volume 17, Edited by Seferlis, P., Georgiadis, C. M., Elsevier Science, Amsterdam, pp. 168-186.

Caballero, J.A., Odjo, A., Grossmann, I.E., 2007. Flowsheet optimization with complex cost and size functions using process simulators. AIChE Journal 53 (9): 2351–2366.

739 Cardoso, M.F., Salcedo, R.L., Feyo de Azevedo, S., Barbosa, D., 2000. Optimization of reactive
740 distillation processes with simulated annealing. Chemical Engineering Science 55 (21) 5059-
741 5078.
742 Carrera-Rodríguez, M., Segovia-Hernández, J.G., Bonilla-Petriciolet, A., 2011. Short-cut method for
743 the design of reactive distillation columns. Industrial & Engineering Chemistry Research 50
744 (18) 10730–10743.
745 Chemical Engineering, 2011. Economic indicators. December: page 69, (Online: http://www.che.com,
746 accessed March 2012).
747 Dimitriadis, V., Pistikopoulos, E. N., 1995. Flexibility analysis of dynamic systems. Industrial &
748 Engineering Chemistry Research 34 (12), 4451–4462.
749 Dragomir, R.M., Jobson, M., 2005. Conceptual design of single-feed hybrid reactive distillation
750 columns. Chemical Engineering Science 60 (16) 4377–4395.
751 Georgiadis, M.C., Schenk, M., Pistikopoulos, E.N., Gani, R., 2002. The interactions of design, control
752 and operability in reactive distillation systems. Computers & Chemical Engineering 26 (4-5)
753 735–746.
754 Georgakis, C., Uztürk, D., Subramanian, S., Vinson, D.R., 2003. On the operability of continuous
755 processes. Control Engineering Practice 11 (8), 859–869.
756 Grossmann, I. E., Floudas, C. A., 1987. Active constraint strategy for flexibility analysis in chemical
757 processes. Computers & Chemical Engineering 11 (6), 675–693.
758 Guttinger T.E., Morari M., 1999a. Predicting multiple steady states in equilibrium reactive distillation.
759 1. Analysis of nonhybrid systems. Industrial & Engineering Chemistry Research 38, 1633-
760 1648.
761 Guttinger T.E., Morari M., 1999b. Predicting multiple steady states in equilibrium reactive
762 distillation. 2. Analysis of hybrid systems. Industrial & Engineering Chemistry Research 38,
763 1649-1665.

764 Huang, H-P, Chien, I-L, Lee, H-Y, 2012. Plantwide control of a reactive distillation process, in:
765 Rangaiah G P, Kariwala V., (Eds.), Plantwide control: recent developments and applications.
766 Chichester: John Wiley 319-338.
767 ICIS pricing, 2012. Online: http://www.icispricing.com, accessed Dec 2011).
768 Jackson, J.R., Grossmann, I.E., 2001. Disjunctive programming approach for the optimal design of
769 reactive distillation columns. Computers & Chemical Engineering 25 (11-12) 1661-1673.
770 Jones, D., Tamiz, M., 2010. Practical goal programming. Springer, New York.
771 Khaledi, R., Young, B.R., 2005. Modeling and model predictive control of composition and
772 conversion in an ETBE reactive distillation column. Industrial & Engineering Chemistry
773 Research, 44 (9) 3134-3145.
774 Konda, N.V.S.N. M., Rangaiah, G.P., Krishnaswamy, P.R., 2006. A simple and effective procedure
775 for control degrees of freedom. Chemical Engineering Science 61, (4), 1184–1194.
776 Lee, H-Y, Lee, Y-C, Chien, I-L, Huang, H-P, 2010. Design and control of a heat-integrated reactive
777 distillation system for the hydrolysis of methyl acetate. Industrial & Engineering Chemistry
778 Research 49 (16) 7398–7411.
779 Luyben, W.L., 2005. Comparison of pressure-swing and extractive-distillation methods for methanol-
780 recovery systems in the TAME reactive-distillation process. Industrial & Engineering
781 Chemistry Research 44 (15) 5715–5725.
782 Luyben, W.L., 2006. Distillation design and control using Aspen simulation. Wiley-Interscience,
783 Hoboken, N.J.
784 Luyben, W.L., Yu, C., 2008. Reactive distillation design and control. John Wiley Hoboken.
785 MATLAB documentation, 2012. Optimization toolbox user's guide. (Online:
786 http://www.mathworks.co.uk/help/pdf_doc/optim/optim_tb.pdf, accessed March 2012)
787 Malcolm, A., Polan, J., Zhang, L., Ogunnaike B. A., Linninger A. A., 2007. Integrating systems
788 design and control using dynamic flexibility analysis. AIChE Journal, 53 (8), 2048–2061.
789 McAvoy, T.J., Arkun, Y., Chen, R., Robinson, D., Schnelle, P.D., 2003. A new approach to defining a
790 dynamic relative gain. Control Engineering Practice 11 (8) 907–914.

791 Miranda, M., Reneaume, J.M., Meyer, X., Meyer, M., Szigeti, F., 2008. Integrating process design
792 and control: An application of optimal control to chemical processes. Chemical Engineering &
793 Processing 47 (11) 2004-2018.
794 Moaveni, B., Khaki-Sedigh, A., 2009. Control Configuration Selection for Multivariable Plants.
795 Springer, Berlin.
796 Morari, M., 1983. Design of resilient processing plants-III: A general framework for the assessment
797 of dynamic resilience. Chemical Engineering Science 38 (2) 1881-1891.
798 Panjwani, P., Schenk, M., Georgiadis, M.C., Pistikopoulos, E.N., 2005. Optimal design and control of
799 a reactive distillation system. Engineering Optimization 37 (7) 733–753.
800 Ramzan, N., Faheem, M., Gani, R., Witt, W., 2010. Multiple steady states detection in a packed-bed
801 reactive distillation column using bifurcation analysis. Computers & Chemical Engineering 34
802 (4) 460–466.
803 Sahinidis, N V., 2004. Optimization under uncertainty: state-of-the-art and opportunities. Computers
804 and Chemical Engineering 28 (6-7), 971–983.
805 Sharifzadeh, M., Rashtchian, D., Pishvaie, M.R., Thornhill, N.F., 2011. Energy induced separation
806 network synthesis of an olefin compression section: A case study. Industrial & Engineering
807 Chemistry Research 50 (3) 1610–1623.
808 Sharifzadeh. M., Thornhill, N.F., 2012. Optimal selection of control structures using a steady-state
809 inversely controlled process model. Computers & Chemical Engineering 38, 126–138.
810 Sharifzadeh. M., Thornhill, N.F., 2013. Integrated design and control using a dynamic inversely
811 controlled process model. Computers & Chemical Engineering 48, 121–134.
812 Sharma, N., Singh K., 2010. Control of reactive distillation column: A review. International Journal of
813 Chemical Reactor Engineering 8 (R5) 1-55.
814 Skogestad S. 2000. Self-optimizing control: the missing link between steady-state optimization and
815 control. Computers & Chemical Engineering 24 (2-7) 569-575.
816 Slotine, J. E., Li, W., 1991. Applied Nonlinear Control. Prentice-Hall, Englewood Cliffs.

Sneesby, M.G., Tade, M.O., Smith, T.N., 2000. A multi-objective control scheme for an ETBE reactive distillation column. Chemical Engineering Research and Design 78 (A2) 283-292.

Solution (121621) Call to DMS_IPOFF3( ) needs to be changed in Aspen Plus 2006 and higher. Aspen Technology, (Online: http://support.aspentech.com/, a secured website accessed March 2012).

Sundmacher, K., Kienle, A., 2003. Reactive distillation: Status and future directions. Wiley-VCH, Weinheim.

Ulrich, G.D., Vasudevan, P.T., 2006. How to estimate utility costs. Chemical Engineering, April 66-69.

Zhang, T., Jensen, K., Kitchaiya, P., Phillips, C., Datta, R., 1997. Liquid-phase synthesis of ethanol-derived mixed tertiary alkyl ethyl ethers in an isothermal integral packed-bed reactor. Industrial & Engineering Chemistry Research 36 4586-4594.

Zhu, F., Huang, K., Wang, S., Shan, L., Zhu, Q., 2009. Towards further internal heat integration in design of reactive distillation columns—Part IV: Application to a high-purity ethylene glycol reactive distillation column. *Chemical Engineering Science*, 64, (15), 3498–3509.

Appendix: Fortran code

The original Fortran code was adapted from Luyben and Yu (2008). In the following, the texts inside the dotted envelopes are the new codes changed by the author in order to update the old Fortran code according to a solution from AspenTech® (Solution 121621).

New code:

```
      SUBROUTINE RAETBELB (NSTAGE, NCOMP,   NR,    NRL,    NRV,
     &                     T,     TLIQ,   TVAP,   P,      VF,
     &                     F,     X,      Y,      IDX,    NBOPST,
     &                     KDIAG,  STOIC,   IHLBAS, HLDLIQ,  TIMLIQ,
     &                     IHVBAS, HLDVAP,  TIMVAP, NINT,    INT,
     &                     NREAL,  REAL,    RATES,  RATEL,   RATEV,
     &                     NINTB,  INTB,    NREALB, REALB,   NIWORK,
     &                     IWORK,  NWORK,   WORK)
      IMPLICIT NONE
      INTEGER NCOMP,  NR,     NRL,    NRV,    NINT,
     &        NINTB,  NREALB,  NIWORK,  NWORK,  N_COMP
      INTEGER K_ETOH, K_IC4,   K_NC4,   K_ETBE
      PARAMETER (K_ETOH=1)
      PARAMETER (K_IC4=2)
```

```
      PARAMETER (K_NC4=3)
      PARAMETER (K_ETBE=4)
      PARAMETER (N_COMP=4)
      INTEGER IDX(NCOMP),  NBOPST(6),    INT(NINT),
     &        INTB(NINTB),  IWORK(NIWORK),  NSTAGE,
     &        KDIAG,       IHLBAS,       IHVBAS,    NREAL,  KPHI,
     &        KER,         L_GAMMA,      J
      REAL*8 X(NCOMP,3),      Y(NCOMP),
     &       STOIC(NCOMP,NR),  RATES(NCOMP),
     &       RATEL(NRL),      RATEV(NRV),
     &       REALB(NREALB),   WORK(NWORK),   B(1),   T,
     &       TLIQ,            TVAP,         P,     VF,   F
      REAL*8 HLDLIQ,   TIMLIQ,   HLDVAP,   TIMVAP,   TZERO,
     &       FT
      REAL*8 DLOG
      INTEGER IMISS, IDBG
      REAL*8 REAL(NREAL), RMISS, C1, C2, C3,
     &       C4,   C5,   C6,     DKA,    DKR,
     &       Q,    RATE, RATNET,  KETBE,  KA,  KRATE
     &      REAL*8 PHI(N_COMP)
     &      REAL*8 DPHI(N_COMP)
     &      REAL*8 ACTIV(N_COMP)
#include "ppexec_user.cmn"
      EQUIVALENCE (RMISS, USER_RUMISS)
      EQUIVALENCE (IMISS, USER_IUMISS)
#include "dms_maxwrt.cmn"
#include "dms_lclist.cmn"
      INTEGER DMS_ALIPOFF3
#include "dms_plex.cmn"
      EQUIVALENCE(B(1),IB(1))
      DATA IDBG/0/
 9010 FORMAT(1X,3(G13.6,1X))
 9000 FORMAT('fugly failed at T=',G12.5,'P=',G12.5,'ker=',I4)
 9020 FORMAT('compo',I3,'mole-frac',G12.5,'activity=',G12.5)
 9030 FORMAT('stage=',I4,'spec-rate=',G12.5,'net-rate=',G12.5)
C
C     BEGIN EXECUTABLE CODE
      KETBE=DEXP(10.387D0+4060.59D0/T-2.89055D0*DLOG(T)-0.0191544D0*T+
     &    5.28586D-5*T**2-5.32977D-8*T**3)
      KA=DEXP(-1.0707D0+1323.1D0/T)
      KRATE=(2.0606D12*DEXP(-60.4D3/8.314D0/T))
      IF(IDBG.GE.1)THEN
        WRITE(MAXWRT_MAXBUF(1),9010) FT,DKA,DKR
        CALL DMS_WRTTRM(1)
      ENDIF
      KPHI=1
C     fugacity coefficient of components in the mixture
      CALL PPMON_FUGLY(T,P,X(1,1)
     &     , Y, NCOMP, IDX, NBOPST, KDIAG, KPHI, PHI, DPHI, KER)
      IF(KER.NE.0)THEN
        WRITE(MAXWRT_MAXBUF(1),9000) T,P,KER
        CALL DMS_WRTTRM(1)
      ENDIF
C     NEW
      L_GAMMA=DMS_ALIPOFF3(24)
      DO J=1,NCOMP
        ACTIV(J)=dexp(B(L_GAMMA+LCLIST_LBLCLIST+J))*X(J,1)
      END DO
      IF(IDBG.GE.1)THEN
       DO J=1,NCOMP
```

```
912           WRITE(MAXWRT_MAXBUF(1),9020) J,X(J,1),ACTIV(J)
913           CALL DMS_WRTTRM(1)
914          END DO
915         ENDIF
916         RATE=REALB(1)*KRATE*(ACTIV(K_ETOH))**2.d0*
917              (ACTIV(K_IC4)-ACTIV(K_ETBE)/KETBE/ACTIV(K_ETOH))
918         RATE=(RATE/(1.D0+KA*ACTIV(K_ETOH))**3.d0)/1.d3
919         RATES(K_IC4)=-RATE
920         RATES(K_ETOH)=-RATE
921         RATES(K_ETBE)=RATE
922         RATES(K_NC4)=0.D+00
923         IF (IDBG.GE.1)THEN
924           WRITE(MAXWRT_MAXBUF(1),9030) NSTAGE,RATE,RATNET
925           CALL DMS_WRTTRM(1)
926         ENDIF
927         RETURN
928     #undef P_MAX3
929         END
```